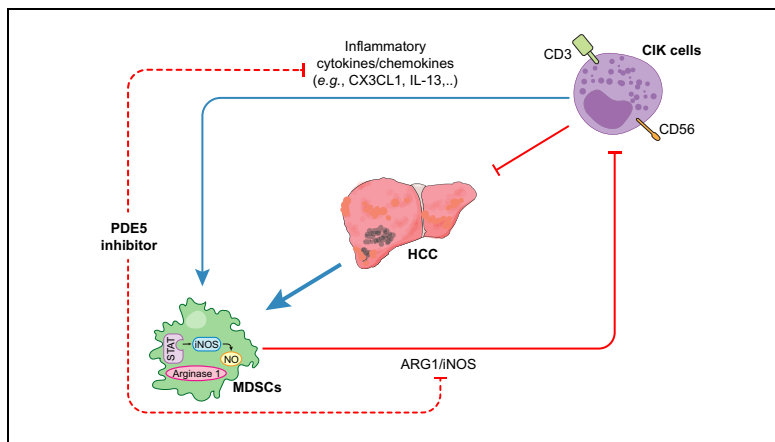


Targeting the crosstalk between cytokine-induced killer cells and myeloid-derived suppressor cells in hepatocellular carcinoma

Graphical abstract



Authors

Su Jong Yu, Chi Ma, Bernd Heinrich, ..., Umberto Rosato, Firouzeh Korangy, Tim F. Greten

Correspondence

tim.greten@nih.gov
(T.F. Greten)

Lay summary

Cytokine-induced killer cells are a mixture of immune cells given to eliminate cancer cells. However, not all patients respond to this treatment. Herein, we show in 2 different liver cancer models that myeloid-derived suppressor cells are increased in response to cytokine-induced killer cell therapy. Targeting these myeloid-derived suppressor cells may provide an additional therapeutic benefit alongside cytokine-induced killer cell therapy.

Highlights

- CIK therapy recruits MDSCs in tumor tissues through inflammatory cytokines.
- MDSCs inhibit CIK tumor lytic function in an ARG1 and iNOS dependent manner.
- Tadalafil, an FDA approved PDE5 inhibitor, suppressed the number and function of MDSCs.
- Tadalafil enhances antitumor efficacy of CIK cells in *in vivo* murine HCC models.
- Human MDSCs inhibit human CIK cell cytotoxicity.



Targeting the crosstalk between cytokine-induced killer cells and myeloid-derived suppressor cells in hepatocellular carcinoma

Su Jong Yu^{1,2}, Chi Ma¹, Bernd Heinrich¹, Zachary J. Brown¹, Milan Sandhu¹, Qianfei Zhang¹, Qiong Fu¹, David Agdashian¹, Umberto Rosato¹, Firouzeh Korangy¹, Tim F. Greten^{1,3,*}

¹Gastrointestinal Malignancy Section, Thoracic and Gastrointestinal Oncology Branch, Center for Cancer Research, National Cancer Institute, National Institutes of Health, Bethesda, MD 20892, USA; ²Department of Internal Medicine and Liver Research Institute, Seoul National University College of Medicine, Seoul, Republic of Korea; ³NCI CCR Liver Cancer Program, USA

Background & Aims: Cytokine-induced killer (CIK) cell-based immunotherapy is effective as an adjuvant therapy in early stage hepatocellular carcinoma (HCC) but lacks efficacy in advanced HCC. We aimed to investigate immune suppressor mechanisms in HCC, focusing on the role of myeloid-derived suppressor cells (MDSCs) in response to CIK therapy.

Methods: MDSCs were quantified by flow cytometry and quantitative real-time PCR. Cytokines were detected by cytokine array. A lactate dehydrogenase cytotoxicity assay was performed in the presence or absence of MDSCs to study CIK function against HCC cells *in vitro*. An FDA-approved PDE5 inhibitor, tadalafil, was used to target MDSCs *in vitro* and *in vivo*. Two different murine HCC cell lines were tested in subcutaneous and orthotopic tumor models in C57BL/6 and BALB/c mice. The anti-tumor effects of human CIKs and MDSCs were also tested *in vitro*.

Results: Adoptive cell transfer of CIKs into tumor-bearing mice induced inflammatory mediators (e.g., CX3CL1, IL-13) in the tumor microenvironment and an increase of tumor-infiltrating MDSCs, leading to impaired antitumor activity in 2 different HCC models. MDSCs efficiently suppressed the cytotoxic activity of CIKs *in vitro*. In contrast, treatment with a PDE5 inhibitor reversed the MDSC suppressor function via ARG1 and iNOS blockade and systemic treatment with a PDE5 inhibitor prevented MDSC accumulation in the tumor microenvironment upon CIK cell therapy and increased its antitumor efficacy. Similar results were observed when human CIKs were tested *in vitro* in the presence of CD14⁺HLA-DR^{-/low} MDSCs. Treatment of MDSCs with a PDE5 inhibitor suppressed MDSC suppressor function and enhanced CIK activity against human HCC cell lines *in vitro*.

Conclusion: Our results suggest that targeting MDSCs is an efficient strategy to enhance the antitumor efficacy of CIKs for the treatment of patients with HCC.

Lay summary: Cytokine-induced killer cells are a mixture of immune cells given to eliminate cancer cells. However, not all

patients respond to this treatment. Herein, we show in 2 different liver cancer models that myeloid-derived suppressor cells are increased in response to cytokine-induced killer cell therapy. Targeting these myeloid-derived suppressor cells may provide an additional therapeutic benefit alongside cytokine-induced killer cell therapy.

Published by Elsevier B.V. on behalf of European Association for the Study of the Liver.

Introduction

Hepatocellular carcinoma (HCC) is a common and fatal cancer, with an increasing incidence worldwide.¹ Though many curative therapies have been developed, the overall response to these therapies is inadequate and the long-term prognosis of patients with HCC remains poor because of its high recurrence rates.² A lot of data have shown that tumor progression is correlated with the accumulation of myeloid-derived suppressor cells (MDSCs) which induce local and possibly systemic immunosuppression.³ Moreover, a greater prevalence of MDSCs has been correlated with early recurrence and was shown to be a predictor of poor prognosis in patients with HCC who underwent curative resection,⁴ radiotherapy,⁵ and hepatic arterial infusion chemotherapy.⁶ MDSCs have been shown to suppress CD8⁺⁷⁻⁹ and CD4⁺ T¹⁰ cells as well as natural killer (NK)¹¹ cells through diverse direct or indirect mechanisms.¹²

Cytokine-induced killer (CIK) cells are a mixed cell population of effector cells with diverse T cell receptor specificities that also possess non-major histocompatibility complex-restricted cytotoxic activity against tumor cells. CIK cells, which comprise cytotoxic T cells, NK cells, and NK-like T cells that express both NK- and T-cell markers are expanded *ex vivo* using recombinant IFN- γ , IL-2 and anti-CD3.¹³ CIK cell-based immunotherapies have been widely studied and used in the treatment of patients with cancer, including HCC.¹⁴ Currently, 90 registered clinical trials are listed on the [ClinicalTrials.gov](http://www.clinicaltrials.gov) website (<http://www.clinicaltrials.gov>) when the following keywords are used in the search: cytokine-induced killer cells or CIK.¹⁵

A recent study determined that adjuvant immunotherapy using CIK cells appeared to reduce the recurrence of HCC and to improve overall survival.¹⁶ Although adjuvant CIK cell-based immunotherapy is a promising treatment option for early stage HCC, it lacks efficacy in advanced HCC.¹⁷⁻¹⁹ We hypothesized that CIK cells could trigger a counter-regulatory immuno-

Keywords: CIK; PDE5 inhibitor; HCC; Immunotherapy; Combination therapy.
Received 3 January 2018; received in revised form 3 October 2018; accepted 31 October 2018; available online 9 November 2018

* Corresponding author. Address: Gastrointestinal Malignancy Section, Thoracic and Gastrointestinal Oncology Branch, Center for Cancer Research, National Cancer Institute, National Institutes of Health, Bethesda, MD 20892, USA. Tel.: +1 301 451 4723; fax: +1 301 480 8780.

E-mail address: tim.greten@nih.gov (T.F. Greten).



suppressive mechanism through recruitment of MDSCs that might hinder CIK cell antitumor activity.

We show that adoptive CIK cell therapy leads to an accumulation of MDSCs in the tumor microenvironment, which in turn suppress CIK function. We demonstrate that a PDE5 inhibitor can not only suppress MDSCs accumulation and function, but also enhance CIK cell-based therapy in murine HCC tumor models. Finally, our murine data were corroborated by human *in vitro* data using human CIK and tumor cells as well as MDSCs treated with a PDE5 inhibitor.

Materials and methods

Cell lines

Two murine (luciferase-expressing RIL-175²⁰ and BNL²⁰) and 2 human (Hep3B²¹ and PLC/PRF/5²¹) HCC cell lines were used in this study.

Drugs

Tadalafil (Selleckchem, TX, USA), a phosphodiesterase-5 (PDE5) inhibitor, was used *in vitro* at a concentration of 100 μ M and was administered by intraperitoneal (i.p.) injection (2 mg/kg/24 h) *in vivo*.²² N-omega-hydroxy-L-arginine (Sigma-Aldrich, MO, USA) and N(G)-monomethyl-L-arginine (Sigma-Aldrich, MO, USA) were added to cell cultures (10 μ M) *in vitro*.

The methods of cell isolation, generation of CIK cells, isolation of MDSCs, flow cytometry analysis, cytotoxicity assays, cytokine array and quantitative real-time PCR are described in the [supplementary information](#).

Animal studies

Male and female C57BL/6 and BALB/c mice were obtained from NCI/Frederick (Frederick, MD, USA). Male B6(Cg)-Tyr-2/J (B6-albino) mice were obtained from Jackson Laboratory (Bar Harbor, USA). All mice were group-housed (5 mice per cage) and were maintained under a 12 h light – 12 h dark cycle with free access to water and standard mouse chow. Subcutaneous tumors were established by injection of 1×10^6 RIL-175 or 1×10^6 BNL cells into the left flank of C57BL/6 or BALB/c mice, respectively. Mice with tumor sizes between 150 and 200 mm³ were randomly assigned to 4 groups with 5 mice per group. Tumor volume was blindly measured using calipers every 3 days and calculated according to the formula: length \times width²/2 mm³. Data are reported as the average tumor size \pm standard error of mean (SEM). To induce orthotopic tumors, 1×10^5 RIL-175 cells in 20 μ l of a 50:50 solution of PBS and Matrigel (or only phosphate buffered saline [PBS] as a control) were injected under the liver capsule into the left lobe of the liver of anesthetized recipient 5-week-old male B6(Cg)-Tyr-2/J (B6-albino) mice after subcostal laparotomy.²⁰ The establishment and growth of tumors were monitored by bioluminescent imaging (BLI) using the Xenogen *in vivo* imaging system (IVIS Spectrum; Caliper Life Sciences, Hopkinton, MA, USA). BLI was blindly performed on days 7, 14, and 21 using the IVIS Spectrum Imaging System as previously reported.²³ Mice were anesthetized with 2% isoflurane in oxygen at 2 L/min. Ten minutes after the mice received an intraperitoneal injection of 150 mg/kg of D-luciferin in PBS, bioluminescence images were acquired with an exposure time of 1–120 s, medium binning, 1f/stop, with an open filter. A region of interest (ROI) was drawn around the tumor, and the bioluminescence signal was quantified as photons/s/cm²/steradian (p/s/cm²/sr).²³ Intrahepatic

orthotopic tumors were allowed to grow for 7 days, at which point the mice were randomized into 4 groups with 5 mice per group according to the bioluminescence signal. Then, based on their group, the mice were administered 5×10^6 CIK cells intravenously in the tail vein and/or a PDE5 inhibitor. Tadalafil (Selleckchem, TX, USA), a PDE5 inhibitor, was administered daily by i.p. injection (2 mg/kg/24 h).²² Mice were maintained under specific pathogen-free conditions and received humane care according to institutional guidelines. Tissues were fixed and stained with anti-Ly6G (clone 6D17, Acris Antibodies GmbH, Germany). The analyses of stained tissues are described in the [supplementary information](#). All experiments were performed according to institutional guidelines and were approved by an NCI-Bethesda (Bethesda, MD, USA) Institutional Animal Care and Use Committee.

Statistical analysis

The sample size for the animal studies was guided by a previous study in our laboratory in which the same C57BL/6 or BALB/c mice strains were used.²⁴ No animals were excluded. Randomization was performed during the *in vivo* study. Measurements were performed in a blind manner whenever possible. Statistical analysis was performed using GraphPad Prism v7.03 (GraphPad Software). The significance of the difference between groups was calculated by Student's unpaired *t* test, 1-way or 2-way ANOVA (Tukey's and Bonferroni's multiple comparison test). Welch's corrections were used when variances between groups were unequal. *p* < 0.05 was considered statistically significant.

Results

CIK cell therapy recruits MDSCs to tumor tissues

We tested the effect of adoptive CIK cell therapy in a murine subcutaneous HCC model using RIL-175-derived tumors. CIK cells were generated from splenocytes of tumor-free C57BL/6 mice ([Fig. S1](#)) and CIK cell therapy was initiated 2 weeks after injection of RIL-175 cells when the tumors were palpable (average tumor volume: 50 mm³). As shown in [Fig. 1A](#), CIK cell therapy caused only marginal inhibition of subcutaneous tumor growth (*p* = 0.0369). We studied the tumor microenvironment by quantitative real-time PCR and noticed an increase in CD11b by quantitative real-time PCR ([Fig. 1B](#)) in liver tumors after adoptive cell therapy with CIK cells. Based on these findings, we performed flow cytometry on tumor-infiltrating immune cells and assessed MDSCs ([Fig. S2](#)). The numbers of both CD11b⁺Ly6G⁺Ly6C^{low} polymorphonuclear (PMN)-MDSCs and CD11b⁺Ly6G⁻Ly6C^{high} monocytic (M)-MDSCs were increased in tumors after adoptive CIK cell therapy (*p* < 0.05, [Fig. 1C](#)). In contrast, a reduction in both CD11b⁺Ly6G⁺Ly6C^{low} PMN-MDSCs and CD11b⁺Ly6G⁻Ly6C^{high} M-MDSCs was observed in the spleens of mice after adoptive CIK cell transfer (*p* < 0.05, [Fig. 1D](#)).

To better understand the mechanism by which MDSCs accumulated in these HCC models upon adoptive CIK cell therapy, we studied cytokines upon co-culture of CIKs with tumor cells and found CX3CL1 and IL-13, which are 2 cytokines that are known to be related to MDSCs trafficking to the tumor site ([Fig. 1E](#)).^{25,26}

MDSCs inhibit the tumor lytic function of CIK cells against HCC

Since adoptive CIK cell therapy showed only limited antitumor effects and since we also observed an increase in the number

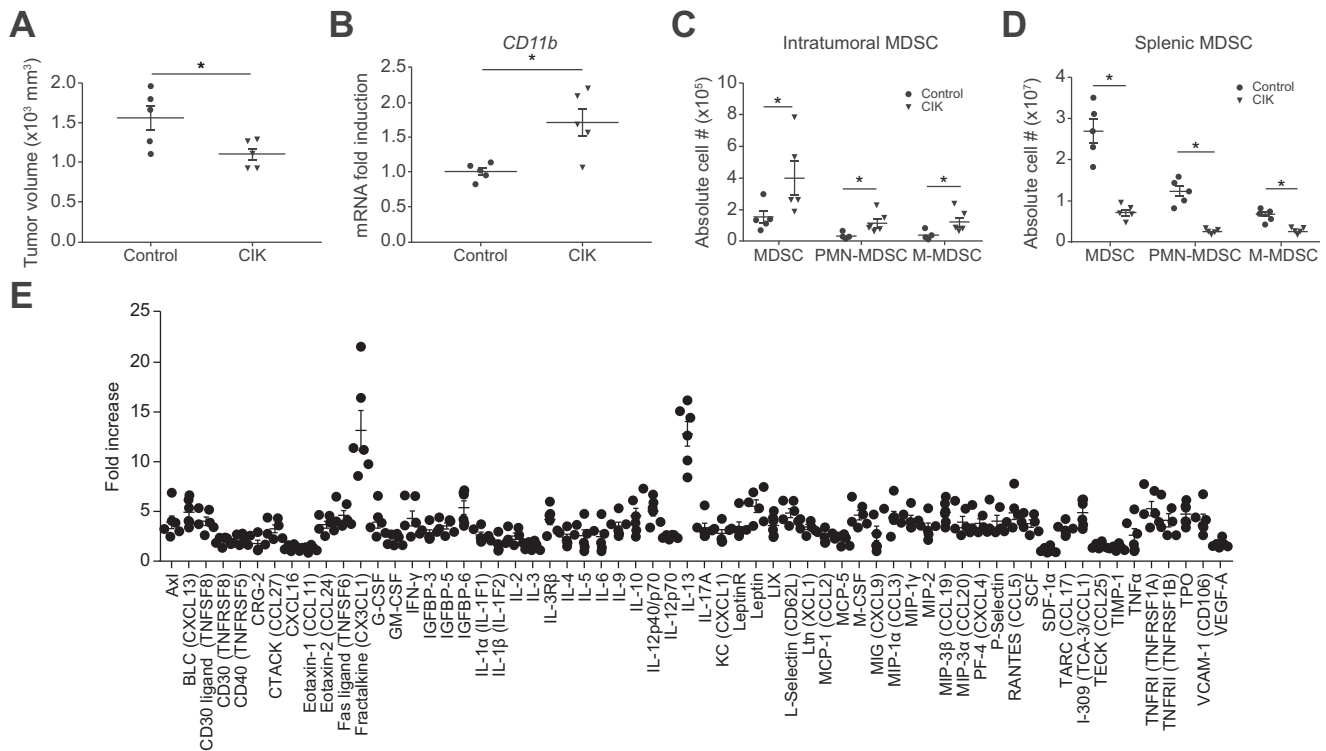


Fig. 1. CIK cell therapy decreases HCC tumor volume but cannot reduce the numbers of intratumoral MDSCs. (A) Male C57BL/6 mice were subcutaneously inoculated with 1×10^6 RIL-175 HCC cells. The size of the tumors in the HCC xenograft mouse models was blindly measured by a caliper. Then, 1 to 2 weeks later, 5×10^6 CIK cells were intravenously injected into the tumor-bearing mice. $n = 5$ for control, $n = 5$ for CIK, Student's *t* test, $*p = 0.0369$. (B) *CD11b* expression was evaluated by quantitative real-time PCR. $n = 5$ for control, $n = 5$ for CIK, Student's *t* test, $*p < 0.05$. The frequency of (C) intratumoral and (D) splenic MDSCs was determined by flow cytometry. Total MDSCs were defined as $CD45^+CD11b^+Gr1^+$ cells, while PMN-MDSCs and M-MDSCs were gated as $CD11b^+Ly6G^+Ly6C^{low}$ and $CD11b^+Ly6G^-Ly6C^{high}$ cells, respectively. The gating strategy from a representative sample is shown in Fig. S2. $n = 5$, Student's *t* test, $*p < 0.05$. Mean \pm SEM. (E) A cytokine array using conditioned media from co-cultured RIL-175 and CIK cells vs. splenocytes as a control. Three independent experiments are shown. CIK, cytokine-induced killer; HCC, hepatocellular carcinoma; M, mononuclear; MDSCs, myeloid-derived suppressor cells; PMN, polymorphonuclear.

of tumor-infiltrating MDSCs upon treatment, we tested whether MDSCs can impair CIK cell cytotoxicity. We generated murine CIK cells from splenocytes of tumor-free C57BL/6 mice (Fig. S1) and isolated murine $CD11b^+Ly6G^+Ly6C^{low}$ PMN-MDSCs and $CD11b^+Ly6G^-Ly6C^{high}$ M-MDSCs from RIL-175 tumor-bearing C57BL/6 mice (Fig. S3). CIK lytic activity was tested against RIL-175 HCC tumor cells in the presence or absence of both MDSC subsets. Naïve splenocytes were used as a control for MDSCs. A dose-dependent suppression of CIK cell cytotoxicity was observed when CIK cells were co-cultured with either PMN-MDSCs or M-MDSCs, even at a 10:1 CIK to MDSCs ratio (Fig. 2A and B). However, no suppression was observed when CIK cells were co-cultured with splenocytes. In addition, MDSCs did not lyse CIK cells or RIL-175 cells at any ratio tested (data not shown). We repeated this experiment using BALB/c mice and a different HCC cell line (BNL cells).²⁰ CIK cells were generated from BALB/c mice (Fig. S4), and PMN- and M-MDSCs were isolated from BNL-tumor-bearing BALB/c mice (Fig. S5). As shown, both MDSC subsets impaired CIK cell cytotoxicity against BNL tumor cells (Fig. S6A and B). Together, our results show that MDSCs efficiently impair the cytotoxicity of CIK cells against 2 different murine HCC cell lines.

Simultaneous ARG1 and iNOS inhibition by tadalafil rescues CIK cell function from suppression by MDSCs

Next, we studied the mechanism by which MDSCs inhibit CIK cell function. The roles of arginase 1 (ARG1) and inducible nitric

oxide synthase (iNOS [NOS2]), which are part of 2 major suppression pathways used by MDSCs, were assessed using N-omega-hydroxy-L-arginine (L-NOHA, an ARG1-specific inhibitor) and/or N(G)-monomethyl-L-arginine (L-NMMA, an iNOS inhibitor). Although treatment with L-NMMA or L-NOHA alone only partially reversed the inhibition of CIK cell cytotoxicity against RIL-175 HCC cells by both MDSC subsets (L-NMMA, 30.1% for PMN-MDSCs and 31.6% for M-MDSCs; L-NOHA, 43.1% for PMN-MDSCs and 29.1% for M-MDSCs), the combined treatment achieved $\sim 51.7\%$ of cytotoxicity (Fig. 3A and B). This suggests that simultaneous ARG1 and iNOS inhibition is a good strategy by which the tumor lytic function of CIK cells may be rescued from suppression by MDSCs.

Tadalafil, a PDE5 inhibitor approved by the FDA, has been shown to suppress MDSC function through the downregulation of both ARG1 and iNOS expression.²² Therefore, we tested the possibility of using a single treatment of tadalafil to block both ARG1 and iNOS and to rescue CIK cell function. Indeed, tadalafil efficiently restored the tumor lytic activity of CIK cells from either PMN-MDSCs or M-MDSCs by achieving up to 51.6% of cytotoxicity (Fig. 3A and B). No additional effect was found when tadalafil was combined with L-NOHA and/or L-NMMA (Fig. 3A and B), which indicates that tadalafil functions through the blockade of ARG1 and iNOS.

We obtained similar results using BNL HCC tumor cells with CIK cells and MDSCs generated from BALB/c mice (Fig. S7A and B), showing this finding was not dependent on mouse strain or a

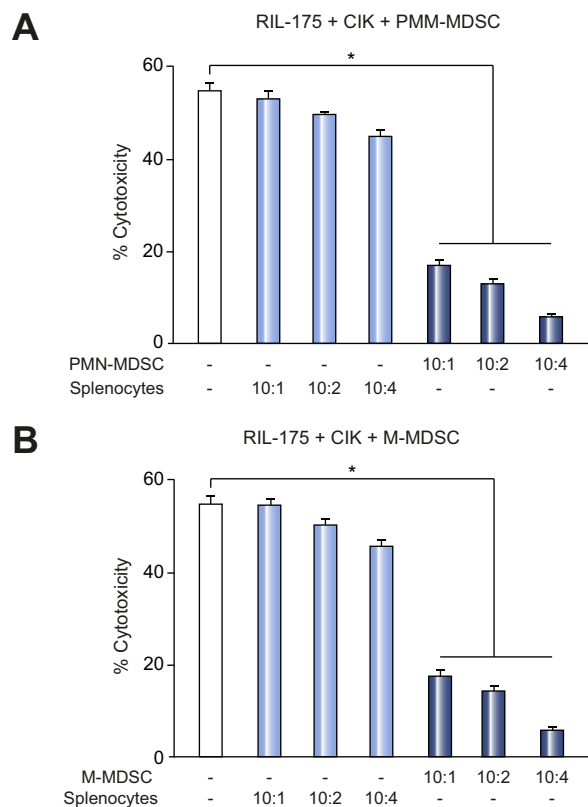


Fig. 2. CD11b⁺Ly6G⁺Ly6C^{low} and CD11b⁺Ly6G⁻Ly6C^{high} cells suppress CIK cell function. Cells were generated or isolated from C57BL/6 mice. CIK cells were incubated with different ratios of (A) CD11b⁺Ly6G⁺Ly6C^{low} PMN-MDSCs or splenocytes, as indicated and (B) CD11b⁺Ly6G⁻Ly6C^{high} M-MDSCs or splenocytes as indicated. After 24 h, RIL-175 cells were added at a ratio of 10:1 (E:T), and lysis was determined by a lactate dehydrogenase cytotoxicity assay. Cumulative results from 3 independent experiments are shown. Mean ± SEM. *p = 0.001. CIK, cytokine-induced killer; M, mononuclear; MDSCs, myeloid-derived suppressor cells; PMN, polymorphonuclear.

specific HCC tumor type. In addition, neither tadalafil, L-NMMA nor L-NOHA had any direct effects on the CIK cell dependent lysis of 2 different HCC murine cell lines (Fig. S8A and B).

Tadalafil simultaneously suppresses the number and function of MDSCs

Next, we tested the effect of tadalafil in a murine subcutaneous HCC model using RIL-175 tumors. Tadalafil therapy was initiated 2 weeks after injection of RIL-175 cells when the tumors were palpable (average tumor volume: 50 mm³). After 5 days of treatment with tadalafil alone, the subcutaneous tumor volumes were similar to those of control mice (Fig. 4A). However, when we studied tumor-infiltrating MDSCs in these mice, the numbers of both CD11b⁺Ly6G⁺Ly6C^{low} PMN-MDSCs and CD11b⁺Ly6G⁻Ly6C^{high} M-MDSCs were significantly decreased in tumors after tadalafil single treatment (p < 0.05, Fig. 4B). Similarly, a reduction in both CD11b⁺Ly6G⁺Ly6C^{low} PMN-MDSCs and CD11b⁺Ly6G⁻Ly6C^{high} M-MDSCs was observed in the spleens of mice after a single tadalafil treatment (Fig. 4C). The assessment of intratumoral MDSC infiltration by quantitative real-time PCR to detect CD11b (p < 0.05, Fig. 4D) revealed a significant reduction in intratumoral MDSCs, which was consistent with the flow cytometric observations.

To better understand the biology of MDSC reduction in the HCC model using RIL-175 tumors, we obtained serum from mice

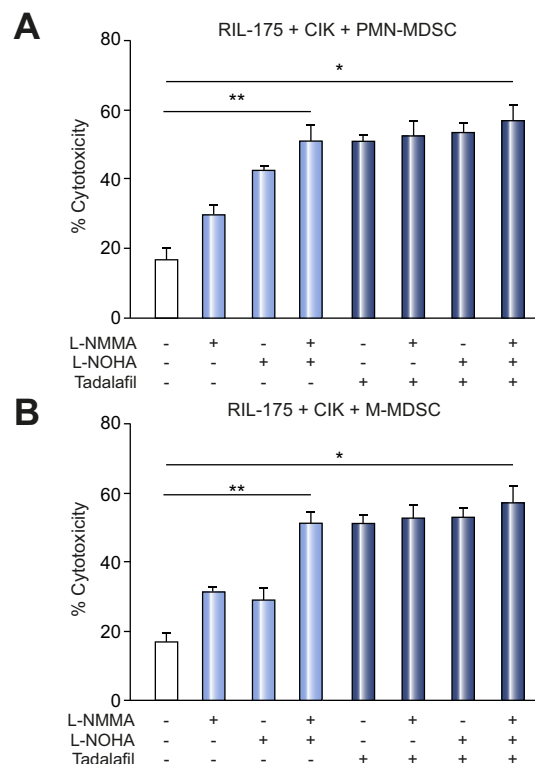


Fig. 3. Inhibition of CIK cell function by MDSCs occurs primarily through arginase and nitric oxide. Cells were generated or isolated from C57BL/6 mice. CIK cells and (A) CD11b⁺Ly6G⁺Ly6C^{low} PMN-MDSCs or (B) CD11b⁺Ly6G⁻Ly6C^{high} M-MDSCs were co-cultured in the presence or absence of N (G)-monomethyl-L-arginine (L-NMMA), N-omega-hydroxy-L-arginine (L-NOHA) (10 μmol/L each), tadalafil (100 μmol/L each), and/or media alone as indicated. After 36 h, RIL-175 cells were added at a ratio of 10:1 (E:T) and lysis was determined by lactate dehydrogenase cytotoxicity assay. CIK cells, purified MDSCs (defined as CD11b⁺Ly6G⁺Ly6C^{low} or CD11b⁺Ly6G⁻Ly6C^{high} cells), and target cells (5,000 cells per well) were co-cultured at a ratio of 10:1:1 (CIK cells: MDSCs: tumor cells). Cumulative results from 3 independent experiments are shown. Mean ± SEM. *p = 0.001. CIK, cytokine-induced killer; M, mononuclear; MDSCs, myeloid-derived suppressor cells; PMN, polymorphonuclear.

5 days after the single tadalafil treatment. Serum was tested in a cytokine array, which revealed a decrease in cytokines, including CX3CL1 and IL-13, in the tadalafil group compared with the control group (Fig. 4E).

In addition, both MDSC subsets isolated from tadalafil-treated mice did not suppress CIK cell cytotoxicity against RIL-175 HCC cells at any ratio tested (Fig. 4F and G).

Tadalafil enhances the antitumor efficacy of CIK cells in vivo

Next, we tested whether tadalafil treatment could be used to enhance the efficacy of CIK cell therapy for HCC in male C57BL/6 mice bearing subcutaneous RIL-175 tumors. Compared with the controls, a single therapy of CIK cells or tadalafil caused only a mild suppression of tumor growth (Fig. 5A and B). In contrast, the combination of tadalafil and adoptive CIK cell therapy led to clear tumor growth inhibition (Fig. 5A and B). Similar results were found in male BALB/c mice bearing subcutaneous BNL tumors (Fig. 5C and D), female C57BL/6 mice (Fig. S9A and B), and female BALB/c mice (Fig. S9C and D). Again, in all the tested tumor models using 2 different HCC murine cell lines, 2 different mouse strains, and male and female mice, a consistent increase in both CD11b⁺Ly6G⁺Ly6C^{low} PMN-MDSCs and

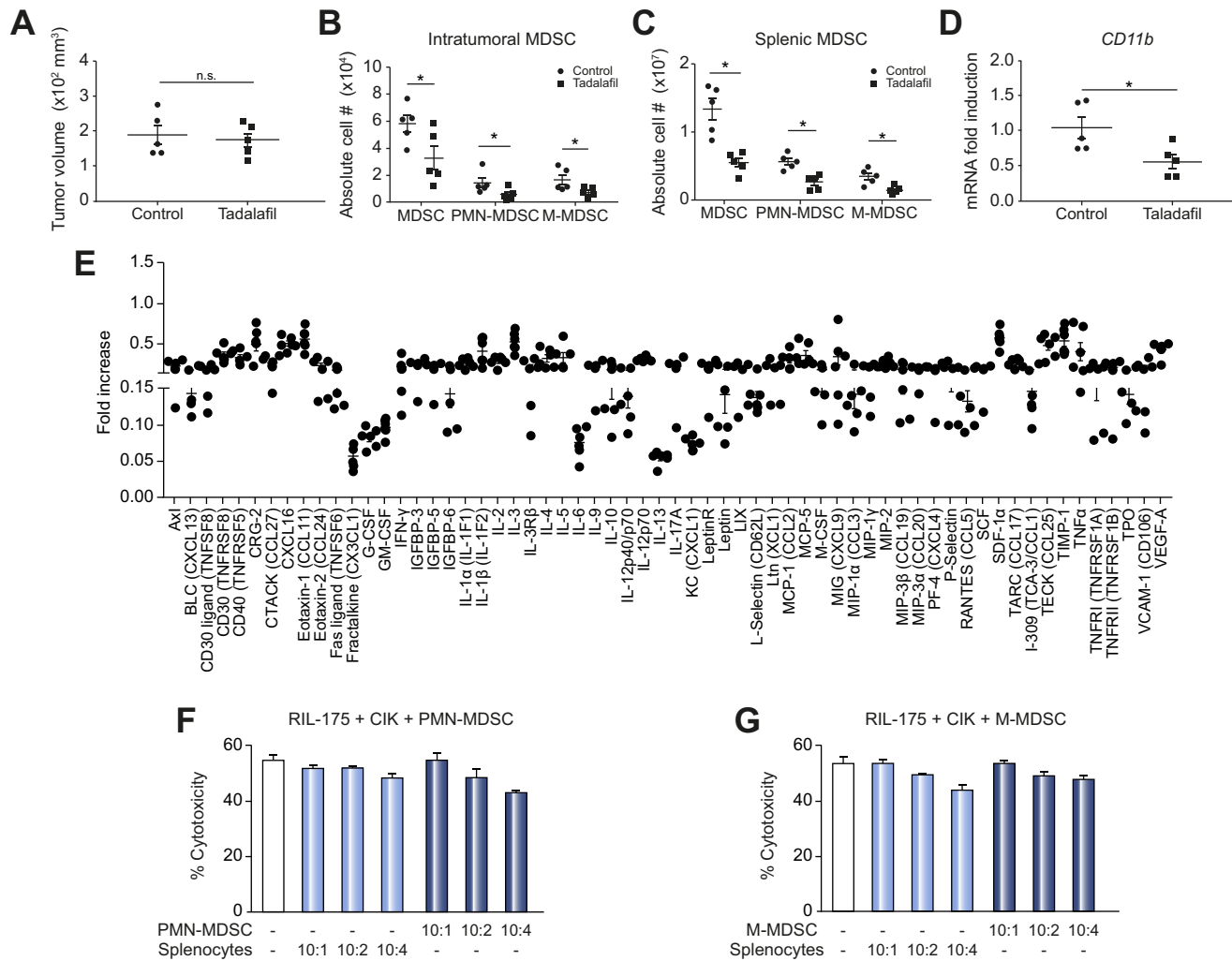


Fig. 4. Tadalafil simultaneously suppresses the number and function of MDSCs. (A) Male C57BL/6 mice were subcutaneously inoculated with 1×10^6 RIL-175 HCC cells. An investigator blinded to experimental treatment group assignments used calipers to measure the tumor size. Then, 1 to 2 weeks later, tadalafil (2 mg/kg), a PDE5 inhibitor, was administered to tumor-bearing mice daily for 5 days by i.p. injection. $n = 5$ for control, $n = 5$ for tadalafil, Student's t test, * $n.s.$ not significant. The frequency of (B) intratumoral and (C) splenic MDSCs was determined by flow cytometry. Total MDSCs were defined as $CD45^+CD11b^+GR1^+$ cells, while PMN-MDSCs and M-MDSCs were gated as $CD11b^+Ly6G^+Ly6C^{low}$ and $CD11b^+Ly6G^-Ly6C^{high}$ cells, respectively. The gating strategy from a representative sample is shown in Fig. S2. $n = 5$, Student's t test, * $p < 0.05$. Mean \pm SEM. (D) CD11b expression was evaluated by quantitative real-time PCR. $n = 5$ for control, $n = 5$ for tadalafil, Student's t test, * $p < 0.05$. (E) A cytokine array compared sera from tadalafil-treated RIL-175 tumor-bearing mice with sera of control mice. Data were expressed relative to control mice. $n = 5$ independent experiments. (F & G) CIK cells were incubated with different ratios of both subsets of MDSCs, which were isolated from tadalafil-treated RIL-175 tumor-bearing mice, as indicated. After 24 h, RIL-175 cells were added at a ratio of 10:1 (E:T), and lysis was determined by lactate dehydrogenase cytotoxicity assay. Cumulative results from 3 independent experiments are shown. Mean \pm SEM. CIK, cytokine-induced killer; HCC, hepatocellular carcinoma; M, mononuclear; MDSCs, myeloid-derived suppressor cells; PMN, polymorphonuclear.

$CD11b^+Ly6G^-Ly6C^{high}$ M-MDSCs levels after CIK cell single therapy was observed in tumor tissues. This increase was reversed by combination therapy with tadalafil (Fig. S10). In contrast to tumor tissues, fewer $CD11b^+Ly6G^+Ly6C^{low}$ PMN-MDSCs and $CD11b^+Ly6G^-Ly6C^{high}$ M-MDSCs were found in the spleen after CIK cell therapy (Fig. S11).

Next, we established an orthotopic HCC model by direct injection of RIL-175 cells into mouse livers to study the effect of immunotherapy in a model that more closely resembles the condition of patients with HCC. We took advantage of the fact that RIL-175 cells express luciferase,²⁷ which enabled us to monitor the growth of liver tumors by *in vivo* imaging. The imaging analysis showed that CIK cells or tadalafil treatment alone inhibited liver tumor progression, which was consistent with the observation in the subcutaneous tumor model. However, the combined treatment with tadalafil plus adoptive cell

therapy with CIK cells elicited the strongest antitumor effect (Fig. 6A and B). At the experimental endpoint, intrahepatic tumor tissues were harvested for further evaluation. As shown, combination treatment (CIK cells + tadalafil) significantly reduced both the liver/body weight ratio and the tumor/liver weight ratio (Fig. 6C and D). We also studied tumor-infiltrating MDSCs. Similar to our findings in subcutaneous tumors, CIK cell treatment caused an induction of both the $CD11b^+Ly6G^+Ly6C^{low}$ PMN-MDSC and $CD11b^+Ly6G^-Ly6C^{high}$ M-MDSC populations in liver tumors (Fig. 6E). In contrast, tadalafil treatment reversed the accumulation of tumor-infiltrating MDSCs in response to CIK cell therapy and provided additional protection against HCC (Fig. 6E). However, similar to our findings in subcutaneous tumor models, MDSCs were decreased in splenic tissues in response to CIK cell therapy (Fig. 6F). Together, the results from 2 different murine HCC cell lines and those

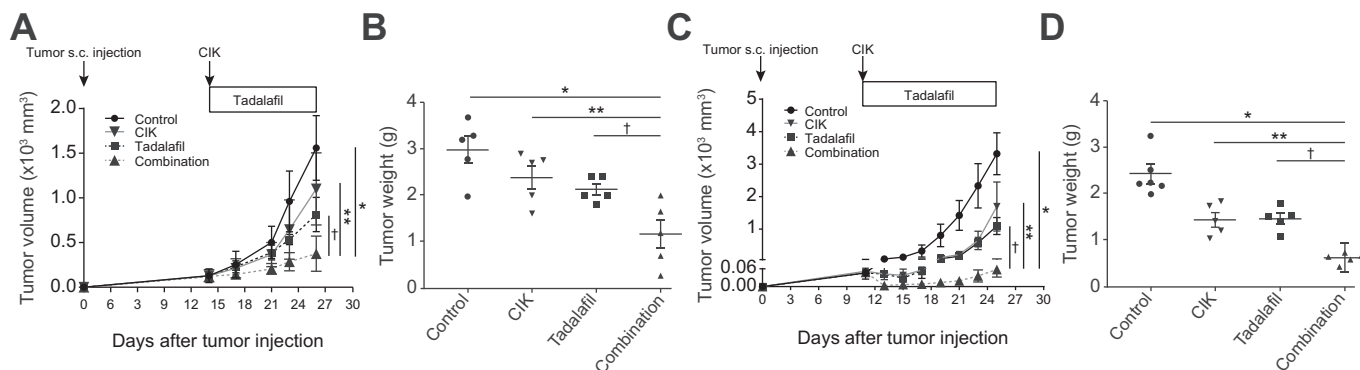


Fig. 5. Tadalafil improves antitumor efficacy of CIK cells against subcutaneous HCC tumors. (A) Male C57BL/6 mice were subcutaneously inoculated with 1×10^6 RIL-175 HCC cells. The sizes of the murine HCC xenograft tumors were blindly measured using a caliper. Then, 1 to 2 weeks later, 5×10^6 CIK cells were intravenously injected into tumor-bearing mice. Tadalafil (2 mg/kg), a PDE5 inhibitor, was administered to the tumor-bearing mice daily by i.p. injection. $n = 5$ for control, $n = 5$ for CIK, $n = 5$ for tadalafil, and $n = 5$ for the combination, 2-way ANOVA, $^*p < 0.0001$ for control vs. combination; $^{**}p < 0.0001$ for CIK vs. combination; $^{\dagger}p = 0.0008$ for tadalafil vs. combination. (B) The weights of the tumor excised from male C57BL/6 mice were measured. $n = 5$ for control, $n = 5$ for CIK, $n = 5$ for tadalafil, and $n = 5$ for the combination, Student's t test, $^*p = 0.0128$ for control vs. combination; $^{**}p = 0.0277$ for CIK vs. combination; $^{\dagger}p = 0.0434$ for tadalafil vs. combination. (C) Male BALB/c mice were subcutaneously inoculated with 1×10^6 BNL HCC cells and experiments were performed as described above. $n = 5$ for control, $n = 5$ for CIK, $n = 5$ for tadalafil, and $n = 5$ for the combination, 2-way ANOVA. $^*p < 0.0001$ for control vs. combination; $^{**}p < 0.0001$ for CIK vs. combination; $^{\dagger}p < 0.0001$ for tadalafil vs. combination. (D) The weights of the tumors excised from male BALB/c mice were measured. $n = 5$ for control, $n = 5$ for CIK, $n = 5$ for tadalafil, and $n = 5$ for the combination, Student's t test, $^*p < 0.0001$ for control vs. combination; $^{**}p = 0.0009$ for CIK vs. combination; $^{\dagger}p = 0.0001$ for tadalafil vs. combination. Mean \pm SEM. CIK, cytokine-induced killer; HCC, hepatocellular carcinoma.

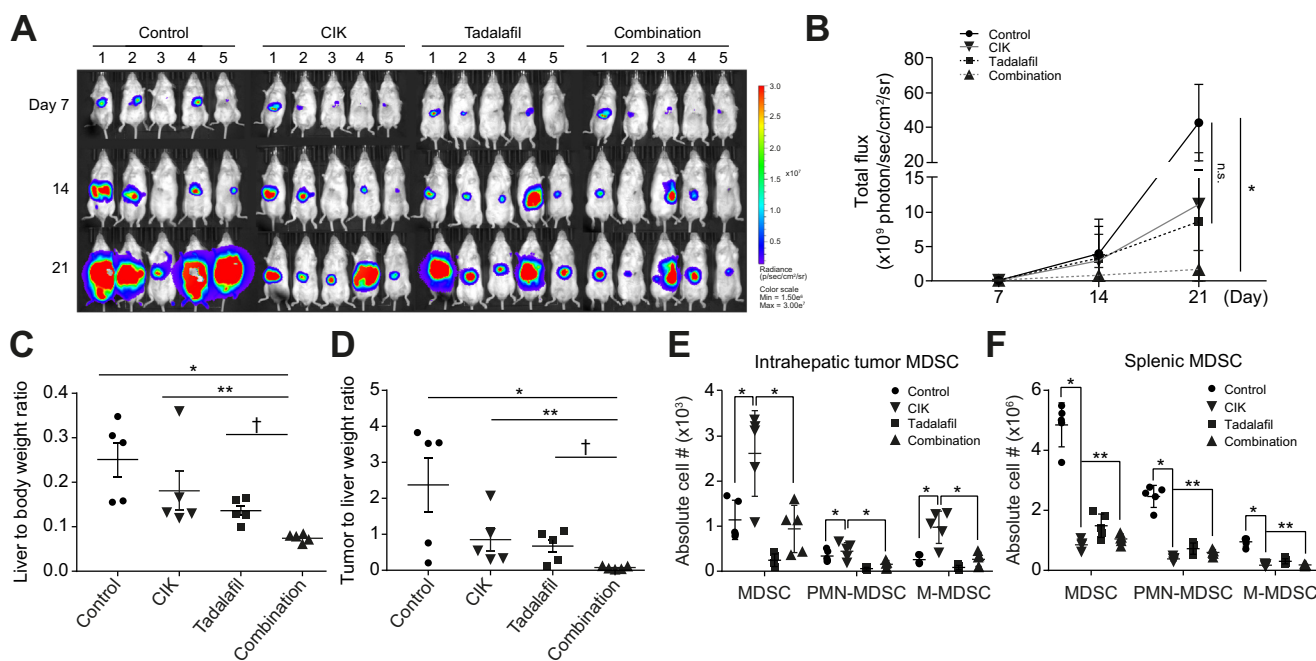


Fig. 6. Tadalafil enhances CIK therapy against an orthotopic HCC model. (A) RIL-175 hepatoma cells ($5 \times 10^5/20 \mu\text{l}$) were orthotopically implanted into the livers of recipient male B6(Cg)-Tyr^{c-2j}/J mice. The establishment and growth of tumors were blindly monitored by BLI with the Xenogen IVIS. BLI represents the proliferation rate through total flux signals of luciferase. The mice were followed-up for 21 days. Tumor-bearing mice were intravenously injected with 5×10^6 CIK cells on day 7. Tadalafil (2 mg/kg), a PDE5 inhibitor, was administered daily to tumor-bearing mice by i.p. injection. (B) Analysis of BLI images was performed by Living Image 2.50 software (PerkinElmer, Waltham, MA, USA). Calculated ROIs are graphed. $n = 5$ for control, $n = 5$ for CIK, $n = 5$ for tadalafil, and $n = 5$ for the combination, 2-way ANOVA. $^*p = 0.0028$ for control vs. combination. (C) The liver/body weight ratio was significantly reduced in the combination treatment (CIK cells + tadalafil) group compared with the other groups. $n = 5$ for control, $n = 5$ for CIK, $n = 5$ for tadalafil, and $n = 5$ for the combination, Student's t test. $^*p = 0.0022$ for control vs. combination; $^{**}p = 0.0011$ for CIK vs. combination; $^{\dagger}p = 0.0465$ for tadalafil vs. combination. (D) The tumor/liver weight ratio was significantly reduced in the combination treatment group compared with the other groups. $n = 5$ for control, $n = 5$ for CIK, $n = 5$ for tadalafil, and $n = 5$ for the combination, Student's t test. $^*p = 0.0184$ for control vs. combination; $^{**}p = 0.0158$ for CIK vs. combination; $^{\dagger}p = 0.0473$ for tadalafil vs. combination. Accumulation of (E) intrahepatic tumoral and (F) splenic MDSCs was determined by flow cytometry. Total MDSCs were defined as CD45⁺CD11b⁺GR1⁺ cells, while PMN-MDSCs and M-MDSCs were gated as CD11b⁺Ly6G⁺Ly6C^{low} and CD11b⁺Ly6G⁺Ly6C^{high} cells, respectively. Student's t test. $^*p < 0.001$ for control vs. CIK. $^{**}p < 0.05$ for CIK vs. combination. Control (black dots; $n = 5$), CIK-treated (purple reverse triangle; $n = 5$), tadalafil-treated (red rectangles; $n = 5$), and combination-treated (blue triangles; $n = 5$) mice. Mean \pm SEM. n.s., not significant. BLI, bioluminescent imaging; CIK, cytokine-induced killer; HCC, hepatocellular carcinoma; M, mononuclear; MDSCs, myeloid-derived suppressor cells; PMN, polymorphonuclear; ROI, region of interest. (This figure appears in colour on the web.)

from subcutaneous and orthotopic tumor models suggest that targeting MDSCs improves the efficacy of CIK cell therapy against HCC.

Human MDSCs inhibit human CIK cell cytotoxicity

To confirm the above findings in human samples, we generated human CIK cells (Fig. S12) and isolated human CD14⁺HLA-DR^{-low} MDSCs (Fig. S13) from peripheral blood mononuclear cells. CD14⁺HLA-DR^{-low} cells significantly suppressed the cytotoxicity of human CIK cells against the human HCC cell lines, Hep3B (Fig. 7A) and PLC/PRF/5 (Fig. 7B), whereas the control CD14⁺HLA-DR⁺ monocytes did not show any significant effect. The inhibition of human CIK cells by human MDSCs (CD14⁺HLA-DR^{-low}) is primarily dependent on ARG1 and iNOS (Fig. 7C and D). As expected, tadalafil restored the tumor lytic function of CIK cells against both Hep3B (Fig. 7C) and PLC/PRF/5 (Fig. 7D) HCC cells. No further abrogation of the suppressive activity of MDSCs against CIK cells by tadalafil was observed in the presence of L-NOHA and/or L-NMMA. Similar to our findings in murine studies, tadalafil, L-NMMA, and L-NOHA had no direct effect on the lytic function of CIK cells when 2 different human HCC cell lines were tested (Fig. S14A and B).

Discussion

With the recent FDA approval of nivolumab for the treatment of patients with HCC who have been previously treated with sorafenib, immunotherapy has become a standard of care treatment option for HCC. Despite encouraging results from different clinical studies of immune checkpoint inhibitors,^{28,29} other types of immunotherapies including adoptive cell therapy remain of great interest.^{30,31} CIK cells have been shown to be active in an adjuvant setting.¹⁶ Here, we studied the immune-mediated mechanism that suppresses the function of CIK-based therapies and tested how the immunosuppressive mechanism can be overcome using drugs already approved by the FDA with the intent to rapidly bring these approaches into the clinic.

In this study, we unexpectedly observed that adoptive CIK cell therapy recruits MDSCs to tumor tissue. Functional studies demonstrated that MDSCs can suppress the lytic function of CIK

cells against HCC through ARG1 and iNOS. With 2 different murine HCC cell lines, subcutaneous and orthotopic tumor models, using 2 different mouse strains, we provide evidence that systemic PDE5 therapy with tadalafil, an FDA-approved drug, improves the antitumor effect of CIK cells against HCC. This is accompanied by a reduction in the number and impairment of the function of tumor-infiltrating MDSCs. Thus, this study suggests that targeting MDSCs is an effective strategy by which the efficacy of CIK cell-based immunotherapy in the treatment of patients with HCC can be improved.

The interest in immunotherapy for the treatment of HCC has recently garnered substantial attention with the approval of nivolumab for the treatment of patients with HCC who have progressed on sorafenib therapy.³² While the primary focus of this particular study was not to examine MDSCs in HCC, it should be noted that single-agent targeting of MDSCs using a PDE5 inhibitor caused a delay in tumor growth in both murine HCC models described here (Figs. 5 and 6). This result suggests that MDSCs not only potently suppress antitumor immunity in HCC but also that targeting these cells may significantly enhance different types of immunotherapy in HCC.

A recent series of prospective randomized trials and retrospective studies showed that adjuvant CIK cell-based immunotherapy can significantly improve prognosis in patients with early stage HCC who have undergone curative treatments including hepatic resection and radiofrequency ablation.^{16,33,34} However, the survival benefits of adjuvant CIK cell-based immunotherapy for patients with advanced-stage HCC remain uncertain.^{18,19} As in many other types of cancer, MDSCs levels increase dramatically during HCC progression,^{25,35-39} and MDSCs inhibit both T cells and NK cells in patients with HCC.^{11,37,40} We propose that suppression of MDSCs using PDE5 inhibitors may represent a new approach to enhance CIK cell-based immunotherapy in HCC. This concept is also supported by studies in other types of cancer, where chemotherapy is routinely used.⁴¹⁻⁴³ In those studies, different types of chemotherapy (gemcitabine, 5-fluorouracil, and oxaliplatin) have been shown to reduce the number of MDSCs and increase the efficacy of CIK cell-based immunotherapy. However, a reduction in MDSCs in those cases may have simply resulted

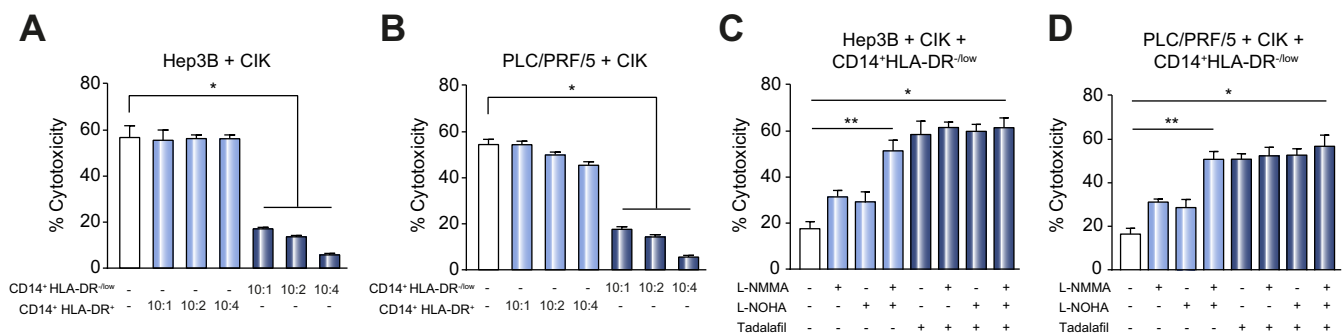


Fig. 7. Tadalafil restores human CIK cell function from MDSCs. Cells were generated or isolated from PBMCs of healthy donors. Human CIK cells were incubated with different ratios of CD14⁺HLA-DR^{-low} cells or CD14⁺HLA-DR⁺ cells as indicated. After 24 h, (A) Hep3B or (B) PLC/PRF/5 cells were added at a ratio of 10:1 (E:T), and lysis was determined by lactate dehydrogenase cytotoxicity assay. Cumulative results from 3 independent experiments are shown. Mean ± SEM. Student's *t* test. **p* = 0.001. Human CIK cells and CD14⁺HLA-DR^{-low} cells were co-cultured in the presence or absence of N(G)-monomethyl-L-arginine (L-NMMA), N-omega-hydroxy-L-arginine (L-NOHA) (10 μmol/L each), tadalafil (100 μmol/L each), and/or media alone, as indicated. After 36 h, (C) Hep3B or (D) PLC/PRF/5 cells were added at a ratio of 10:1 (E:T), and lysis was determined by lactate dehydrogenase cytotoxicity assay. Human CIK cells, purified human MDSCs (defined as CD14⁺HLA-DR^{-low} cells), and target cells (10,000 cells per well) were co-cultured at a ratio of 10:1:1 (CIK cells: MDSCs: tumor cells). Cumulative results from 3 independent experiments are shown. Mean ± SEM. Student's *t* test. **p* = 0.001. CIK, cytokine-induced killer; HCC, hepatocellular carcinoma; MDSCs, myeloid-derived suppressor cells.

from successful chemotherapy and tumor shrinkage, which would have led to a small number of MDSCs.

Here, our study provides direct pre-clinical evidence that simultaneous reduction in MDSC number and function by an FDA-approved PDE5 inhibitor improved CIK cell-based therapy for HCC. Moreover, this information will help clinicians design better clinical trials to test CIK cell-based therapies in patients with HCC.

One major finding was the observed increase in MDSC numbers in the tumor tissues of mice upon adoptive transfer of CIK cells (Figs. 1D and 6E). A similar observation has been described in adoptive T cell therapy.⁴⁴ It has been speculated that cytokines and/or chemokines released in response to adoptive CIK cell therapy recruit MDSCs to the tumor tissues. It remains to be determined which factors, if any, might affect the recruitment of MDSCs after CIK cell therapy. However, clearly, CX3CL1 and IL-3 play an important role in the accumulation of MDSCs at the tumor site, which was associated with CIK cell therapy in this study.^{25,26} One limitation of our murine models is that subcutaneous tumors do not reflect the situation of HCC that arises in the liver. To overcome this limitation, we established an orthotopic HCC model to better mimic the condition of patients with HCC.

Although we have shown that a PDE5 inhibitor, tadalafil, suppressed MDSCs in an iNOS- and ARG1-dependent manner, the full mechanism that underlies these effects remains to be elucidated. One putative mechanism involves the impact of these inhibitors on mRNA stability. cGMP destabilizes iNOS mRNA by reducing the ubiquitous mRNA binding protein, human antigen R.⁴⁵ The other possibility is that high levels of cGMP induced by a PDE5 blockade reduce the cytosolic Ca²⁺ concentration,⁴⁶ which leads to a reduction in the activity of calcium-dependent protein kinase C,⁴⁷ this in turn prevents the upregulation of IL-4R α and ARG1.⁴⁸

Further work is required to elucidate the exact mechanism by which MDSCs suppress CIK cells. Additional studies are also needed to determine whether CIK cells can also affect MDSCs in patients with HCC. The multifaceted role of MDSCs further illustrates the complexity of the immune-suppressive mechanisms in patients with HCC, and consequently, the necessity to design new CIK cell-based immunotherapies that target these pathways.

In summary, our study has uncovered a novel mechanism of immune evasion for HCC tumors whereby MDSCs regulate adoptive immunotherapy and its effector cells, the CIK cells. Impaired CIK cells can in turn affect the antitumor immune responses, which further contributes to tumor escape from CIK cell-based immunotherapy in patients with advanced HCC.

Financial support

The authors are supported by the Intramural Research Program of the NIH, NCI (ZIA-BC-011345) and a grant from the Liver Research Foundation of Korea (Bio Future Strategies Research Project).

Conflict of interest

The authors declare they have no conflicts of interest.

Please refer to the accompanying ICMJE disclosure forms for further details.

Authors' contributions

SJ.Y, B.H., and Z.J.B. performed experiments, while SJ.Y., C.M., B.H., Z.J.B., F.K., and T.F.G. analyzed data. M.S., Q.Z., Q.F., D.A., and U.R. assisted with experiments. SJ.Y. and T.F.G. conceived and designed the project, while SJ.Y. and T.F.G. wrote the manuscript. All authors contributed to writing and all provided feedback.

Acknowledgement

We would like to thank Dr. Jung-Hwan Yoon and the Berzofsky lab for their helpful discussion.

Supplementary data

Supplementary data to this article can be found online at <https://doi.org/10.1016/j.jhep.2018.10.040>.

References

Author names in bold designate shared co-first authorship

- [1] El-Serag HB, Kanwal F. Epidemiology of hepatocellular carcinoma in the United States: where are we? Where do we go? *Hepatology* 2014;60:1767–1775.
- [2] Chen WT, Chau GY, Lui WY, Tsay SH, King KL, Loong CC, et al. Recurrent hepatocellular carcinoma after hepatic resection: prognostic factors and long-term outcome. *Eur J Surg Oncol* 2004;30:414–420.
- [3] Serafini P, Borrello I, Bronte V. Myeloid suppressor cells in cancer: recruitment, phenotype, properties, and mechanisms of immune suppression. *Semin Cancer Biol* 2006;16:53–65.
- [4] **Gao XH, Tian L**, Wu J, Ma XL, Zhang CY, Zhou Y, et al. Circulating CD14+ HLA-DR-/low myeloid-derived suppressor cells predicted early recurrence of hepatocellular carcinoma after surgery. *Hepato Res* 2016.
- [5] Wang D, An G, Xie S, Yao Y, Feng G. The clinical and prognostic significance of CD14(+)/HLA-DR(-/low) myeloid-derived suppressor cells in hepatocellular carcinoma patients receiving radiotherapy. *Tumour Biol* 2016;37:10427–10433.
- [6] Mizukoshi E, Yamashita T, Arai K, Terashima T, Kitahara M, Nakagawa H, et al. Myeloid-derived suppressor cells correlate with patient outcomes in hepatic arterial infusion chemotherapy for hepatocellular carcinoma. *Cancer Immunol Immunother* 2016;65:715–725.
- [7] Gabrilovich DI, Velders MP, Sotomayor EM, Kast WM. Mechanism of immune dysfunction in cancer mediated by immature Gr-1+ myeloid cells. *J Immunol* 2001;166:5398–5406.
- [8] Bronte V, Chappell DB, Apolloni E, Cabrelle A, Wang M, Hwu P, et al. Unopposed production of granulocyte-macrophage colony-stimulating factor by tumors inhibits CD8+ T cell responses by dysregulating antigen-presenting cell maturation. *J Immunol* 1999;162:5728–5737.
- [9] Kusmartsev S, Nefedova Y, Yoder D, Gabrilovich DI. Antigen-specific inhibition of CD8+ T cell response by immature myeloid cells in cancer is mediated by reactive oxygen species. *J Immunol* 2004;172:989–999.
- [10] Nagaraj S, Gabrilovich DI. Regulation of suppressive function of myeloid-derived suppressor cells by CD4+ T cells. *Semin Cancer Biol* 2012;22:282–288.
- [11] **Hoechst B, Voigtlaender T**, Ormandy L, Gamrekelashvili J, Zhao F, Wedemeyer H, et al. Myeloid derived suppressor cells inhibit natural killer cells in patients with hepatocellular carcinoma via the Nkp30 receptor. *Hepatology* 2009;50:799–807.
- [12] Haile LA, Greten TF, Korangy F. Immune suppression: the hallmark of myeloid derived suppressor cells. *Immunol Invest* 2012;41:581–594.
- [13] Jiang J, Wu C, Lu B. Cytokine-induced killer cells promote antitumor immunity. *J Transl Med* 2013;11:83.
- [14] **Cai XR, Li X**, Lin JX, Wang TT, Dong M, Chen ZH, et al. Autologous transplantation of cytokine-induced killer cells as an adjuvant therapy for hepatocellular carcinoma in Asia: an update meta-analysis and systematic review. *Oncotarget* 2017;8:31318–31328.
- [15] **Gao X, Mi Y**, Guo N, Xu H, Xu L, Gou X, et al. Cytokine-induced killer cells as pharmacological tools for cancer immunotherapy. *Front Immunol* 2017;8:774.

- [16] Lee JH, Lee JH, Lim YS, Yeon JE, Song TJ, Yu SJ, et al. Adjuvant immunotherapy with autologous cytokine-induced killer cells for hepatocellular carcinoma. *Gastroenterology* 2015;148, 1383–1391.e1386.
- [17] Lee DH, Nam JY, Chang Y, Cho H, Kang SH, Cho YY, et al. Synergistic effect of cytokine-induced killer cell with valproate inhibits growth of hepatocellular carcinoma cell in a mouse model. *Cancer Biol Ther* 2017;18:67–75.
- [18] Takayama T, Sekine T, Makuuchi M, Yamasaki S, Kosuge T, Yamamoto J, et al. Adoptive immunotherapy to lower postsurgical recurrence rates of hepatocellular carcinoma: a randomised trial. *Lancet* 2000;356:802–807.
- [19] Pan QZ, Wang QJ, Dan JQ, Pan K, Li YQ, Zhang YJ, et al. A nomogram for predicting the benefit of adjuvant cytokine-induced killer cell immunotherapy in patients with hepatocellular carcinoma. *Sci Rep* 2015;5:9202.
- [20] Kapanadze T, Gamrekelashvili J, Ma C, Chan C, Zhao F, Hewitt S, et al. Regulation of accumulation and function of myeloid derived suppressor cells in different murine models of hepatocellular carcinoma. *J Hepatol* 2013;59:1007–1013.
- [21] Kamiya T, Chang YH, Campana D. Expanded and activated natural killer cells for immunotherapy of hepatocellular carcinoma. *Cancer Immunol Res* 2016;4:574–581.
- [22] Serafini P, Meckel K, Kelso M, Noonan K, Califano J, Koch W, et al. Phosphodiesterase-5 inhibition augments endogenous antitumor immunity by reducing myeloid-derived suppressor cell function. *J Exp Med* 2006;203:2691–2702.
- [23] Hwang GL, van den Bosch MA, Kim YI, Katzenberg R, Willmann JK, Paulmurugan R, et al. Development of a high-throughput molecular imaging-based orthotopic hepatocellular carcinoma model. *Cureus* 2015;7 e281.
- [24] Ma C, Kesarwala AH, Eggert T, Medina-Echeverez J, Kleiner DE, Jin P, et al. NAFLD causes selective CD4(+) T lymphocyte loss and promotes hepatocarcinogenesis. *Nature* 2016;531:253–257.
- [25] Gabitass RF, Annels NE, Stocken DD, Pandha HA, Middleton GW. Elevated myeloid-derived suppressor cells in pancreatic, esophageal and gastric cancer are an independent prognostic factor and are associated with significant elevation of the Th2 cytokine interleukin-13. *Cancer Immunol Immunother* 2011;60:1419–1430.
- [26] Sevko A, Umansky V. Myeloid-derived suppressor cells interact with tumors in terms of myelopoiesis, tumorigenesis and immunosuppression: thick as thieves. *J Cancer* 2013;4:3–11.
- [27] Kapanadze T, Medina-Echeverez J, Gamrekelashvili J, Weiss JM, Wiltrott RH, Kapoor V, et al. Tumor-induced CD11b(+) Gr-1(+) myeloid-derived suppressor cells exacerbate immune-mediated hepatitis in mice in a CD40-dependent manner. *Eur J Immunol* 2015;45:1148–1158.
- [28] Sangro B, Gomez-Martin C, de la Mata M, Inarrairaegui M, Garralda E, Barrera P, et al. A clinical trial of CTLA-4 blockade with tremelimumab in patients with hepatocellular carcinoma and chronic hepatitis C. *J Hepatol* 2013;59:81–88.
- [29] Duffy AG, Ulahannan SV, Makorova-Rusher O, Rahma O, Wedemeyer H, Pratt D, et al. Tremelimumab in combination with ablation in patients with advanced hepatocellular carcinoma. *J Hepatol* 2017;66:545–551.
- [30] Butterfield LH, Ribas A, Dissette VB, Lee Y, Yang JQ, De la Rocha P, et al. A phase I/II trial testing immunization of hepatocellular carcinoma patients with dendritic cells pulsed with four alpha-fetoprotein peptides. *Clin Cancer Res* 2006;12:2817–2825.
- [31] Palmer DH, Midgley RS, Mirza N, Torr EE, Ahmed F, Steele JC, et al. A phase II study of adoptive immunotherapy using dendritic cells pulsed with tumor lysate in patients with hepatocellular carcinoma. *Hepatology* 2009;49:124–132.
- [32] Greten TF, Sangro B. Targets for immunotherapy of liver cancer. *J Hepatol* 2018;68:157–166.
- [33] Hui D, Qiang L, Jian W, Ti Z, Da-Lu K. A randomized, controlled trial of postoperative adjuvant cytokine-induced killer cells immunotherapy after radical resection of hepatocellular carcinoma. *Dig Liver Dis* 2009;41:36–41.
- [34] Pan K, Li YQ, Wang W, Xu L, Zhang YJ, Zheng HX, et al. The efficacy of cytokine-induced killer cell infusion as an adjuvant therapy for postoperative hepatocellular carcinoma patients. *Ann Surg Oncol* 2013;20:4305–4311.
- [35] Diaz-Montero CM, Salem ML, Nishimura MI, Garrett-Mayer E, Cole DJ, Montero AJ. Increased circulating myeloid-derived suppressor cells correlate with clinical cancer stage, metastatic tumor burden, and doxorubicin-cyclophosphamide chemotherapy. *Cancer Immunol Immunother* 2009;58:49–59.
- [36] Solito S, Falisi E, Diaz-Montero CM, Doni A, Pinton L, Rosato A, et al. A human promyelocytic-like population is responsible for the immune suppression mediated by myeloid-derived suppressor cells. *Blood* 2011;118:2254–2265.
- [37] Hoechst B, Ormandy LA, Ballmaier M, Lehner F, Kruger C, Manns MP, et al. A new population of myeloid-derived suppressor cells in hepatocellular carcinoma patients induces CD4(+)CD25(+)Foxp3(+) T cells. *Gastroenterology* 2008;135:234–243.
- [38] Arihara F, Mizukoshi E, Kitahara M, Takata Y, Arai K, Yamashita T, et al. Increase in CD14+HLA-DR-/low myeloid-derived suppressor cells in hepatocellular carcinoma patients and its impact on prognosis. *Cancer Immunol Immunother* 2013;62:1421–1430.
- [39] Kalathil S, Lugade AA, Miller A, Iyer R, Thanavala Y. Higher frequencies of GARP(+)CTLA-4(+)Foxp3(+) T regulatory cells and myeloid-derived suppressor cells in hepatocellular carcinoma patients are associated with impaired T-cell functionality. *Cancer Res* 2013;73:2435–2444.
- [40] Gabrilovich DI, Nagaraj S. Myeloid-derived suppressor cells as regulators of the immune system. *Nat Rev Immunol* 2009;9:162–174.
- [41] Wang Z, Liu Y, Zhang Y, Shang Y, Gao Q. MDSC-decreasing chemotherapy increases the efficacy of cytokine-induced killer cell immunotherapy in metastatic renal cell carcinoma and pancreatic cancer. *Oncotarget* 2016;7:4760–4769.
- [42] Jiang J, Xu N, Wu C, Deng H, Lu M, Li M, et al. Treatment of advanced gastric cancer by chemotherapy combined with autologous cytokine-induced killer cells. *Anticancer Res* 2006;26:2237–2242.
- [43] Wu C, Jiang J, Shi L, Xu N. Prospective study of chemotherapy in combination with cytokine-induced killer cells in patients suffering from advanced non-small cell lung cancer. *Anticancer Res* 2008;28:3997–4002.
- [44] Hosoi A, Matsushita H, Shimizu K, Fujii S, Ueha S, Abe J, et al. Adoptive cytotoxic T lymphocyte therapy triggers a counter-regulatory immunosuppressive mechanism via recruitment of myeloid-derived suppressor cells. *Int J Cancer* 2014;134:1810–1822.
- [45] Pilz RB, Casteel DE. Regulation of gene expression by cyclic GMP. *Circ Res* 2003;93:1034–1046.
- [46] Rotella DP. Phosphodiesterase 5 inhibitors: current status and potential applications. *Nat Rev Drug Discov* 2002;1:674–682.
- [47] Webb BL, Hirst SJ, Giembycz MA. Protein kinase C isoenzymes: a review of their structure, regulation and role in regulating airways smooth muscle tone and mitogenesis. *Br J Pharmacol* 2000;130:1433–1452.
- [48] Vellenga E, Dokter W, Halie RM. Interleukin-4 and its receptor; modulating effects on immature and mature hematopoietic cells. *Leukemia* 1993;7:1131–1141.